Precursor Processing Development for Low Cost, High Strength Carbon Fiber for Composite Overwrapped Pressure Vessel Applications

Matthew C. Weisenberger (Primary Contact), E. Ashley Morris
University of Kentucky Center for Applied Energy Research
2540 Research Park Drive
Lexington, KY 40511
Phone: (859) 257-0322
Email: Matt.Weisenberger@uky.edu

DOE Manager: Zeric Hulvey, (202) 586-1570, Zeric.Hulvey@ee.doe.gov
Contract Number: DE-EE0008095
Project Start Date: September 1, 2017
Project End Date: December 31, 2020

ACKNOWLEDGEMENT:

This material is based upon work supported by the U.S. Department of Energy's Office of Energy Efficiency and Renewable Energy (EERE) under the Hydrogen and Fuel Cells Technology Office (HFTO) Award Number DE-EE0008095.

Overall Objectives

Carbon fiber (CF) is central to produce lightweight, high pressure, composite overwrapped pressure vessels (COPVs), which are used for on-board storage of hydrogen for fuel cell vehicles. In 2015, carbon fiber cost accounted for 62% of the cost of a hydrogen storage system, as COPVs were manufactured with T700S CF at $29.40/kg CF [1]. The high cost of hydrogen storage, largely attributed to the carbon fiber cost, limits the application of fuel cells in vehicles. Therefore, our team endeavored to develop fiber processing to demonstrate carbon fiber tensile properties similar to T700S with a production cost potential of $12.60/kg or less. Here, the overarching goal of the project was the development of low cost, high strength carbon fiber for composite overwrapped pressure vessels. Within the project, our team investigated a new low-cost, high-volume, high quality polyacrylonitrile (PAN)-based precursor terpolymer for the production of carbon fiber precursors, methods for increasing water and energy use efficiency in wash-water/solvent separation, and ultimately developed a multifilament spinning and conversion process for the production of hollow carbon fibers from a segmented arc spinneret utilizing a solution spinning method.

Technical Barriers

This project addresses the following technical barriers from the Hydrogen Storage section of the Fuel Cell Technologies Office Multi-Year Research, Development, and Demonstration Plan:

- System Weight and Volume
- System Cost
- Materials of Construction

Technical Targets

Table 1. Progress Towards Meeting Technical Targets for Hydrogen Storage for Light-Duty Fuel Cell Vehicles

Characteristic	Units	DOE 2020 Hydrogen Storage Targets	Project Status (initial CF cost of $29.40/kg)
Storage system cost CF cost [2]	$/kg CF	12.60[1] (57.1 % reduction)	12 to 15 is possible (49 to 59 % reduction)

[1] per DE-FOA-0001647

Project Go/No-Go Decision Points

G1: Demonstrate ≥100 filament, air gap spinning of the small diameter TechPAN precursor polymer, followed by oxidization, carbonization and characterization of the resultant carbon fiber. Demonstrate single filament carbon fiber properties approaching 4.9 GPa strength and 230 GPa modulus (similar to T700S). Achieve < 1 wt.% residual solvent in fiber with minimal residence time for the water minimization strategy. Deliver cost analysis showing a reduction of ≥10%, from $29.40/kg to $26.46/kg is possible via low cost polymer.

G2: Demonstrate ≥10 filament, air gap, hollow fiber spinning of TechPAN precursor polymer with OD <100 um and ID <50 um with specific strength and modulus approaching 635 MPa/g/cc and 8.5 GPa/g/cc. Demonstrate lower energy solvent recovery through sorption in activated carbon modules with capability to capture > 50% of the solvent effluent, and their thermal regeneration with <15% loss in specific surface area. Deliver a cost analysis showing a reduction of ≥19%, from $29.40/kg to $23.82/kg is possible by means of low cost polymer, water minimization and low energy solvent recovery.

G3: (End of Project Goal) Demonstrate hollow carbon fiber tensile properties approaching 4.9 GPa strength and 230 GPa modulus (similar to T700S), with an analysis of specific strength pertaining to part weight consideration, and deliver a cost analysis of the precursor and carbon fibers with a cost potential of $12.60/kg.

Proving of low cost, high-volume, high quality polyacrylonitrile (PAN)-based precursor terpolymer

Central to the success of the program was the use of the novel terpolymer polyacrylonitrile polymer, TechPAN, for the spinning of carbon fiber precursors. Supplied by Technorbital with a cost potential of $3/kg, this polymer was not tied to a specific brand or carbon fiber manufacturer and was available to new entry players in the carbon fiber market, significantly lowering the barrier to entry (typical exclusive, aerospace grade PAN polymer costs $7.05/kg [3], and requires immense capex for self-supply). Utilizing 100 filament air gap spinning, TechPAN precursor fibers were produced (shown in **Figure 1**) and converted to carbon fiber (CF) utilizing an efficient strain controlled thermal conversion apparatus capable of applying programmed strain as a function of time (and temperature) for the small-scale conversion of TechPAN precursors to CF. TechPAN precursor was shown in BP1 to be capable of generating tensile properties of T700S CF (4.9 GPa strength, 230 GPa modulus). Filaments were observed with tensile strengths equal to or exceeding 4.9 GPa at 10 mm gauge lengths, and with moduli exceeding 230 GPa. This demonstrated that the low cost TechPAN-derived CF could offer a lower cost, and brand-independent path to T700S properties in CF. This represented a path to lower the final carbon fiber cost by **13%**.

Figure 1. Typical spool of multifilament continuous TechPAN precursor fibers, with round, 10 μm fiber cross sections shown in the inset. A typical spool contained 1 km of multifilament tow length.

Improved water and energy use efficiency

A significant, overlooked cost in the production of high quality, solution-spun precursor fiber is the recovery of solvent and clean water from wash water. Conventional recovery systems currently used in carbon fiber plants employ distillation of millions of gallons of wastewater, incurring an enormous amount of energy and cost[2]. It has been estimated that there are approximately 40 kg (10.6 gal) of wash water generated per kg of PAN precursor. Here, the use of low energy adsorption de-watering was evaluated to concentrate the solvent for recovery via an activated carbon (AC) recovery system. It was determined that the selected commercially available activated carbon was capable of adsorbing approximately 1 g of the spinning solvent, dimethylsulfoxide (DMSO), for every 3 g of AC. This performance was indeed much better than expected. The data gathered during this project found that the use of AC reduced fresh water usage by up to 86%. A 58% capture of solvent effluent by the AC sorption system surpassed the 50% target and milestone (Go/No-Go 2). Moreover, concerning total effluent in our scaled-down spinning system, only 2.8 L of wash water (containing up to 3.1 wt.% DMSO) was recirculated at 300 ml/min with the AC sorption system over a 100 min spin run. By comparison, a similar flow of fresh wash water (as used in plants currently) generated 30 L of wash water at a concentration of 0.58 wt.% DMSO. Both effluent streams would require treatment by distillation to recover the solvent and treat to the water. This represented a 90% reduction in total effluent to distillation.

This said, thermal regeneration of the DMSO-sorbed activated carbon, in our labs, showed a 2.4% loss in AC specific surface area per regeneration cycle. The target was < 15 %, therefore achieving the Go/No-Go 2 targets for water minimization and low energy solvent recovery. Based on our calculations, the use of activated carbon sorption during precursor fiber spinning would reduce the resulting CF cost by $2.36/kg, or 8% largely via reduced energy costs associated with distillation of less solvent-water waste. However, to achieve this level of cost reduction, the regenerability of the AC needed to have approached only 0.02% adsorption capability loss per regeneration cycle. Given the intensive nature of this study, and the desire to focus solely on the development of the hollow carbon fiber concept, reviewer feedback from the 2019 AMR indicated a desire for the team to move forward from Task 3.0 Energy Efficient Solvent Recovery and Water Use and to focus on the hollow fiber work.

---

[2] Latent heat energy of water vaporization is 2.37 kWh/gal ($131,535 / Mgal in energy costs at $0.0555/kWh)

Development of hollow carbon fibers

To reach the $12.60/kg CF target cost from a baseline cost of $29.40/kg CF, the development of hollow carbon fiber (HCF) utilizing a segmented arc spinneret and a solution spinning approach allowed for staying close to time-tested (with existing capital) precursor processing but introduced a bold new direction of hollow multifilament tow processing. To achieve dramatic cost reduction, we proposed to produce hollow precursor fiber, largely on the basis that: (1) hollow precursor fiber would allow for significantly faster thermal processing (particularly during oxidation), and that (2) the majority of the stress in the fiber is concentrated in the outer surface region – due to the relatively disordered core region of solid fiber [4]. Preservation of the solid carbon fiber tensile properties in a lower linear density HCF would allow for identical composite fabrication, but utilize less kilograms of carbon fiber compared to solid carbon fiber. In this project, the hollow precursor fibers allowed for an increased rate of densification during oxidation compared a solid fiber of similar outer diameter and has the potential to avoid to the formation of the undesirable skin-core structure commonly found in commercial CF such as T700S [4, 5]. While segmented arc spinnerets are most commonly used for the production of melt spun hollow filaments, our team developed a methodology to enable their use in solution spinning. When using a segmented arc spinneret, the lumen is supported by a gas (typically air), which enters through the fiber fissure/heal-points, near the spinneret face, as shown in **Figure 2a**. This fissure then heals in the air gap to form the hollow filament, as shown in **Figure 2b**. One attraction of this approach is that it could easily transition to multi-thousand filament tow spinning at existing plants for production of HCF.

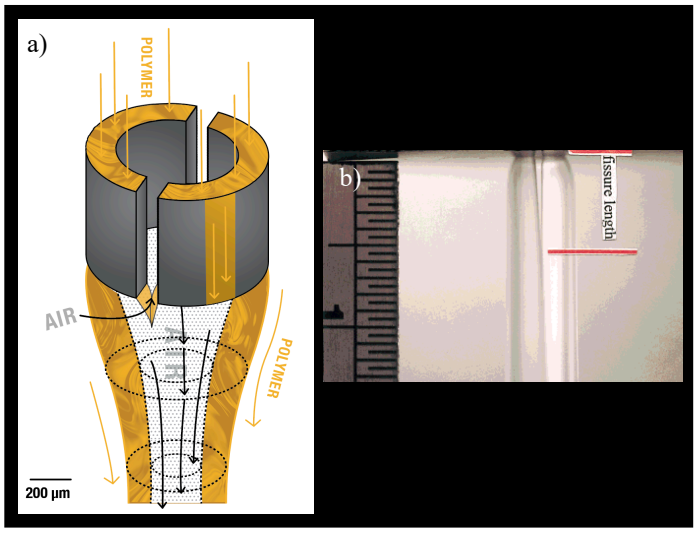

Figure 2. (a) Schematic depicting the use of a segmented arc spinneret (2C) to spin hollow fiber. The two "C"s of extrudate heal in the air gap. Above their heal point, air is sucked into the hollow filament assisting its formation. (b) An example of the use of a segmented arc spinneret showing the "healing" of the two "C"s during the spinning of hollow polypropylene fiber [6].

Hollow precursor fiber development

The production of HF precursors from a segmented arc spinneret was controlled by several variables, including air gap distance, coagulation bath composition, dope flow rate, and draw ratios.

When utilizing a segmented arc spinneret, the segments exiting the capillary require sufficient time to heal to form the hollow fiber, but not so much as to collapse. Initial trials were not successful in producing HF precursors. Throughout initial experimentation, it was discovered that coagulation bath composition was a highly impactful variable in the production of round, concentric HF precursor. Utilizing a 100% water coagulation bath allowed for the stable production of concentric HF precursors without collapse. It was hypothesized that when instantaneous de-mixing occurred, as when spinning into a 100% water bath, a thin cuticle formed on the exterior of the HF, providing resistance to collapse as solvent exchange continued in the bath. A representative 100 m spool of 25 filament hollow PAN precursor fiber is shown in **Figure 3a**. The resulting HF possessed a concentric hole position and uniform wall thickness (**Figure 3b**). However, as a result of coagulation in 100% water, macrovoids formed within the fiber walls, as shown by the red arrow in **Figure 3c**. Initially these voids were attributed to insufficient healing of the 2C segments. However, macrovoids in radially random positions and sometimes greater than two per cross section were observed in any given fiber. This led to the conclusion that the coagulation process was responsible for macrovoid formation, during which the fiber cuticle can rupture under the pressure of inward non-solvent diffusion [7].

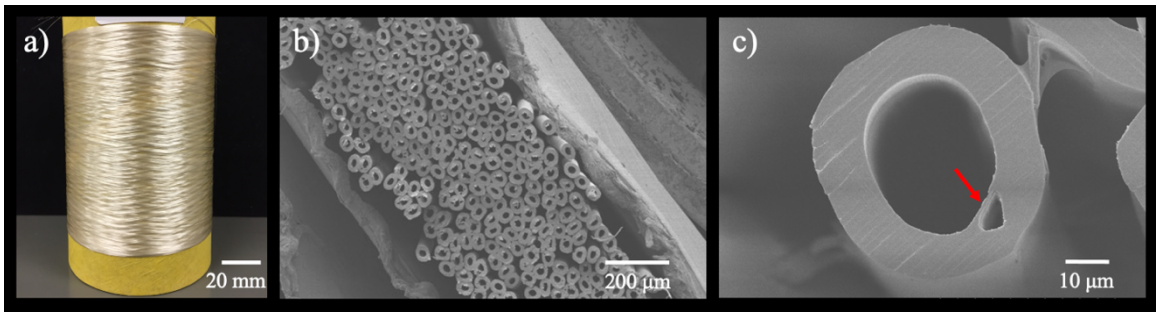

Figure 3. PAN precursor hollow filaments. a) A 100 m spool of 25 filament tow hollow PAN precursor fiber. (b) SEM micrograph showing the cross section of a bundle of hollow precursor fibers. c) SEM micrograph of HF cross section showing a macrovoid.

Tensile properties of several hollow precursor fibers are shown in **Figure 4** as a function of outer diameter (OD). Tensile results for run 516 (based on HF OD) are circled in yellow. The fibers measured 39.5 µm OD and 12.5 µm ID (13.5 µm wall thickness). For N = 16, the effective stress at break was 485 ± 56 MPa and the effective elastic modulus was 11 ± 0.7 GPa. For specific properties, calculated based on a 1.06 g/cc fiber density (based on OD and a bulk density for PAN of 1.18 g/cc), the specific strength was 0.46 N/tex and specific modulus was 10 N/tex. As shown, further decreases in fiber outer diameter improved the tensile properties of the precursor fiber. Although no direct causality can be prescribed between precursor fiber and resultant carbon fiber tensile properties, carbon fiber tensile improvement is generally consistent with decreasing precursor fiber dimensions.

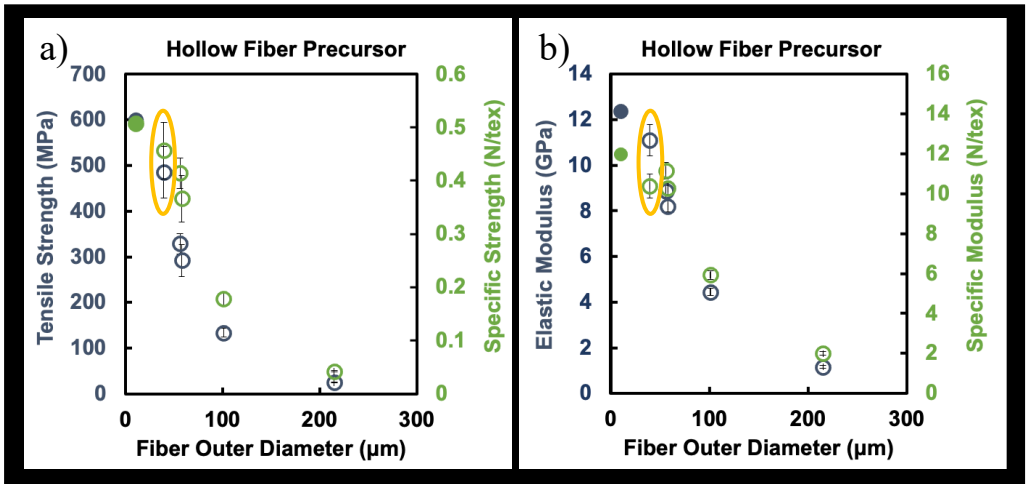

Figure 4. Hollow precursor fiber a) effective tensile strength as a function of outer diameter and b) effective elastic modulus as a function of outer diameter.

As the project progressed, and equipped with greater understanding and control of other major variables such as air gap distance, draw ratio, dope flow rate, dope composition, etc., studies focused on increasing the coagulation bath solvent composition for prevention of macrovoid formation. Fibers were successfully spun using a 10, 20, and 30 wt.% DMSO/water coagulation bath. A drastic reduction in macrovoid content as well as a retention of the hollow fiber form was observed in the 30 wt.% DMSO/water spun fibers. In addition, some HF suffered from inter-filament fusion issues stemming from the spinning process, but this was remedied by the addition of a spin finish prior to hot water stretching.

Oxidation of hollow fibers

Following precursor development, batch oxidative stabilization of precursor HF was completed, and the fibers analyzed. **Figure 5** shows various images of stabilized fibers. In **Figure 5a**, the HF cross section was analyzed using EDX for oxygen content, where oxygen is shown in blue. Higher oxygen content was observed near the outer and inner surfaces in similar thickness bands. This suggested that oxygen diffused in and reacted with the stabilizing PAN from both the fiber exterior and lumen. **Figure 5b** shows an optical micrograph of a HF which was stabilized in a nitrogen atmosphere, where negligible optical contrast through the wall was observed. Fibers shown in **Figure 5c**, **5d**, and **5e** were stabilized in air, similarly to **Figure 5a**. Here, we propose that the relatively brighter regions of increased reflectance are associated with conjugated bonding structures in the ladder PAN formed via oxidative dehydrogenation. This brighter "skin" can be seen (indicated by a light gray skin and a dark gray core). These results are similar to those found by EDX in **Figure 5a** and by other researchers utilizing optical microscopy [8, 9]. The lack of significant conjugation in the core can be explained by the inability of oxygen to diffuse to the core completely during the stabilization process. The solid oxidized fibers in **Figure 5c** had a precursor diameter of 12 μm (spun in-house from the same polymer and under similar processing condition), similar to the wall thickness of the HF (12 μm) in **Figure 5d**, and possessed a skin-core structure. For homogeneous oxygen diffusion, the diffusion length for the solid fiber was 6 μm (the fiber radius). However, **Figure 5c** indicates that the thickness of the skin layer was approximately 4 μm.

Interestingly, the HF in **Figure 5d** also appeared to possess a "skin-core" structure, albeit in the fiber wall. This is magnified in **Figure 5e**, where the higher reflectivity associated with reaction with oxygen from the interior and exterior (lighter gray region) is equivalent, also measuring approximately 4 µm. This left a darker gray core region of 4 µm into which oxygen was unable to completely diffuse, as has been found by other researchers [10, 11]. Of course, this skin-core structure, now found in the HF wall, is still undesirable. However, these results suggest that reducing the wall thickness to 8 µm would allow for complete, homogeneous oxidation of the HF. Even still, these findings illustrate that these HFs experienced oxygen diffusion from the outside and from the inside, simultaneously.

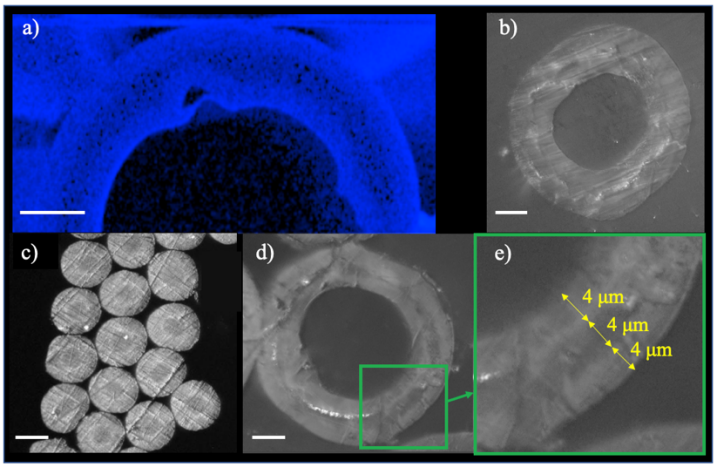

*white scale bars are 10 µm

Figure 5. EDX and optical microscopy (OM) images of stabilized HF and solid fiber (white scale bars are 10 µm). (a) EDX of oxidized HF for oxygen content (oxygen shown in blue); (b) OM image of nitrogen stabilized HF showing no skin-core structure due to the absence of oxygen during heat treatment; (c) OM images of oxidized solid fiber with diameter similar to the wall thickness of the oxidized HF found in (d). (e) OM image of HF wall demonstrating skin-core structure.

Throughout the project, precursor fibers of varying percent open areas were produced. A study was conducted to determine the effect of percent open area on oxidation progression, studying the oxidation of 11% to 44% open area HF. It was found, as expected, that the outer oxidized layer thickness remained constant despite the percent open area of the fiber. What was interesting, however, was that this layer thickness measured approximately 4 µm in thickness for varying diameter fibers (similar to the results shown in **Figure 5**). Yu et al. also found that the oxidized layer thickness for PAN fibers remained at 4 µm despite changing solid fiber diameters [9]. Finally, while the outer oxidized layer thickness remained constant, the inner thickness increased with percent open area, supporting the hypothesis that inner oxidation is dependent on the lumen volume and the air contained within. To achieve a 4 µm inner layer thickness, the data suggested a HF with an approximately 50% open area was necessary. Additionally, to avoid the formation of a skin-core structure, the wall thickness of the HF should be approximately 8 µm or less. Additionally, sets of fibers of varying percent open area with both open and closed ends (closed by embedding fiber ends in epoxy) were evaluated following oxidation. This experiment was designed to determine if air was pulled into the hollow fiber lumen during oxidation. The resulting fibers demonstrated no

difference in inner oxidized layer thickness, indicating that air was not pulled into the lumen during oxidation and that inner oxidation was limited to the volume of air contained within the lumen.

To further explore the impact of HF on oxidation, the rate densification for a hollow fiber was compared to a solid fiber, with, as much as possible, all-else-equal between the fibers. It was hypothesized that an increased oxidation (and therefore densification) rate would occur in the HF because the open area of the hollow allows for oxidation to occur from the interior and exterior of the fiber. Results for the relative rate of fiber density increase during oxidation are shown in **Figure 6** as a function of sampling point during the oxidation process. Oxidized fiber density is known to follow oxygen content, and a target oxidized fiber density (containing the appropriate amount of oxygen to produce high quality carbon fibers) has been suggested to be in the range of 1.34 to 1.39 g/cc [12, 13]. Fiber densities for HF (58 μm OD, 33 μm ID, 12.5 μm wall thickness) as a function of sampling point along the stabilization process were compared to densities for a typical diameter solid TechPAN fiber (11 μm) as well as to a large diameter solid TechPAN fiber (54 μm), both of which were spun in-house from the same polymer under similar processing conditions. Assuming a starting density of 1.18 g/cc, the percent increase in fiber density, relative to the initial precursor fiber density, after each oxidation stage was calculated and plotted in **Figure 6**. A linear fit was applied to the data for each fiber and the slope was used as a proxy for the effective rate of density increase through the oxidation process. As shown in **Figure 6**, the rate of density increase was highest for the 11 μm solid fiber (slope of 5.80) and was lowest for the 54 μm solid fiber (slope of 2.88). The slope of the HF fiber density increase was 3.67. Given the large OD of HF (58 μm), one would expect the rate of densification to have been close to that of the solid 54 μm fiber. However, its faster densification rate is hypothesized to be attributed to the contribution of air (O_2) contained within the lumen. This initial data supports the hypothesis that a HF will increase in density faster compared to a solid fiber of similar outer diameter.

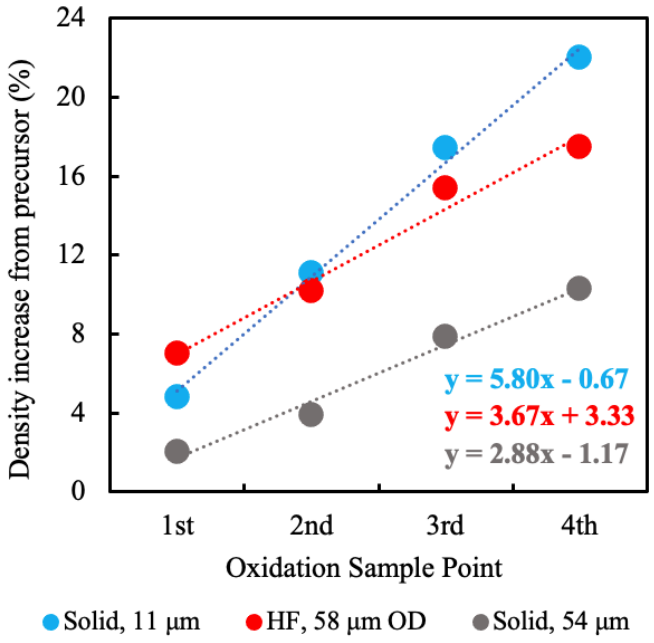

Figure 6. Comparison of densification rate during the oxidative stabilization process for a 11 μm diameter solid precursor fiber, 54 μm diameter solid precursor fiber, and hollow precursor fiber (HF, OD = 58 μm, ID = 33 μm, wall thickness = 12 μm).

LightMat Collaboration for Continuous HF Oxidation

UK collaborated with ORNL (who received LightMAT funding assistance) allowing UK access to ORNL facilities and expertise. In particular, this funding allowed for the use of ORNL continuous oxidation and carbonization processing. As described earlier, UK oxidation and carbonization was carried out in a batch process. However, to better replicate commercial processing of continuous filaments, the ORNL continuous thermal conversion systems were utilized. When continuously oxidizing HF, it was found that the fibers retained their hollow structure despite the rigors of continuous processing, which involved subjecting the fibers to high strains while passing over numerous rollers. The analysis of long lengths (~100 m) of continuously oxidized fiber also allowed for observations of differences between fiber samples taken from the "ends" of the 100 m length and from the center of the fiber length (~50 m from the end). When analyzing the "middle" and "end" samples, it was found that the density in the middle of the spool was 1.3811 ± 0.0121 g/cc compared to 1.3310 ± 0.0047 g/cc at the end of the spool (N=20). It is possible that the sampled ends of the fiber spool were too close to the actual tow end, which would have been involved in string up of the oven system and therefore did not experience the full oxidation process. Other samples further from the tow end would need to be analyzed to verify this result. It is important that we measured a sufficient density (1.3811 g/cc) in the middle of the tow, as this indicates the inner surface of the fiber was not starved for air far from the ends. End and middle samples were analyzed under optical microscopy, shown in **Figure 7**. Similar to **Figure 5**, a light grey "skin" and dark grey "core" are shown in the walls of the oxidized fiber. When observing the sample images, it was difficult to discern differences between the middle and end samples. Both showed evidence of oxidation from the interior and exterior of the filament, but the degree to which this occurs is difficult to determine without further analysis. Key takeaways from the ORNL collaboration through LightMAT funding are that the HF retained its hollow structure despite the rigors of continuous oxidation and that oxidation occurred from the interior and exterior of the filament along the fiber length at length scales of 100s of meters.

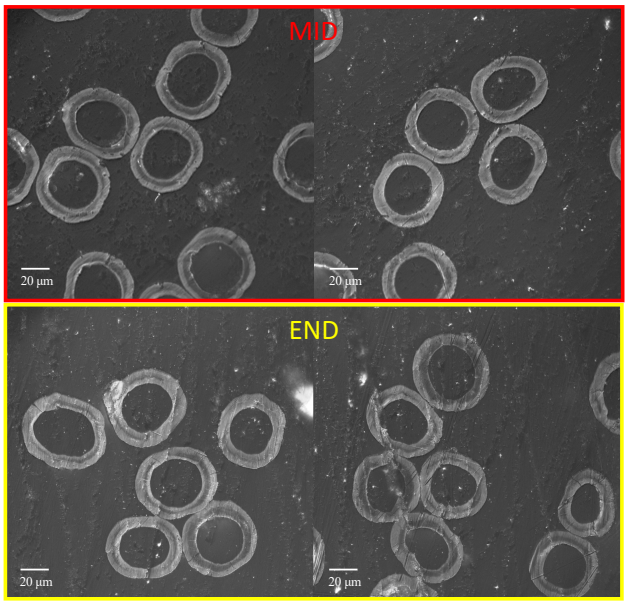

Figure 7. Optical microscopy of oxidized fibers sampled from ORNL continuously oxidized fiber tow at the end of the fiber tow and from the middle of the length of fiber tow.

Carbonization of hollow fibers

Following successful oxidation, the oxidized hollow fibers were carbonized in a batch process via the hanging of various masses from the fibers while under thermal treatment. The resulting HCF retained their hollow structure and their tensile properties were evaluated. The HCF with the highest tensile properties to date as well as a representative SEM image of the HCF are shown in **Figure 8**. These HCF (sourced from the same precursor HF) were carbonized with 0, 50, 100, and 200 gf applied. The resulting HCF had a 35 µm OD, 25 µm ID, and 5 µm wall thickness. The effective tensile properties were determined using the area based on the OD of the fiber and included the lumen area. Interestingly, little change was seen in the effective break strength at 0, 50, and 100 gf, with all HCF measuring ~ 590 MPa. A step change occurred under 200 gf, with the resulting HCF demonstrating an effective tensile strength of 880 MPa, the highest tensile strength HCF observed in the project. Effective modulus saw moderate increases with hanging mass, increasing from 110 GPa at 0 gf to 142 GPa at 200 gf (modulus values are compliance corrected). At 200 gf, the highest tensile strain was attained, at 0.6%. Clearly, more work is needed to achieve the properties of T700S. However, it should be noted that, at 35 µm OD, the HCF reported here were quite large relative to T700S. Reduction in filament dimensions will almost certainly result in significantly increased tensile performance. Although it remains technically challenging, we believe it is achievable to spin much smaller hollow precursor filaments.

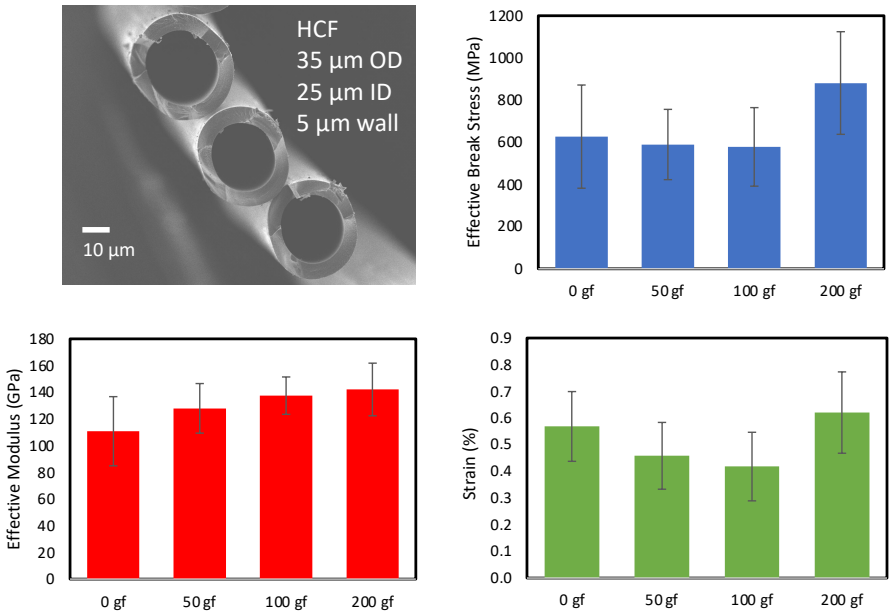

Figure 8. The highest tensile property HCF produced to date, attained by varying the masses applied to the HF during carbonization.

Impact on carbon fiber cost

A recent publication containing carbon fiber cost modeling was published by Choi et al. [14] and we utilized this model for our cost estimates, which breaks down the cost of several of the processing steps in the production of CF and results in a total cost of $25.70/kg CF. The fiber manufacturing costs are shown in **Table 2**. As stated previously, the hollow structure of the fiber allowed oxidation to proceed from both the interior and exterior of the fiber. Our results demonstrated a 30% faster oxidation of large diameter hollow precursor relative to a solid baseline (Figure 6). With smaller outer diameter fiber we predict the densification rate advantage of the hollow fiber to improve. Assuming we can speed the oxidation process by 2.1x with smaller precursor hollow filaments, and commensurately increase the through-oven line speed, significant cost reduction in HCF production could be realized. A 14 µm OD, 9.3 µm ID hollow precursor fiber, with 44% open, the total plant throughput (mass of HCF produced per time) would increase by 18% as outlined in Table 2.

Table 2. CF manufacturing costs. The HF process targets a 7/4.65 OD/ID µm final CF (44% open): A 2.1x increase in line speed from oxidation through post treatment, enables an 18% increase in overall CF throughput with a 16.8% cost savings (in $/kg carbon fiber).

Choi, D., et al. *Carbon* 2019, 142, 610-649		44% open HF Processing: with line speed increase = 2.1x	
Process	**Baseline Cost $/kg CF**	**Cost $/kg HCF**	**0.56x tow linear density x 2.1x line speed = 1.18x Increase in plant throughput**
Precursor Polymer	$9.17	$6.60	$3/kg TechPAN vs. $4.17/kg baseline polymer*
Wet Spinning	$4.83	$4.83	Spinning process cost/kg CF largely unchanged
Oxidation	$4.82	$4.10	2.1x line speed = 1.18x throughput
Carbonization	$4.00	$3.40	2.1x line speed = 1.18x throughput
Post Treatment	$2.88	$2.45	2.1x line speed = 1.18x throughput
Sum	**$25.70**	**$21.38**	
% savings		16.8%	

*2.2 kg precursor polymer per 1 kg CF

Also, the exothermic heat of reaction limits the tow band thickness through oxidation, which if unchecked can cause fires. With this 44% lower linear density tow, the web thickness could likely and safely double, relative to solid fiber processing. In this case, a mere 5% increase in line speed through conversion would also yield 16.8% savings in $/kg CF. Moreover, for new plants, smaller oxidation systems could be utilized with lower capital & operating costs.

The most powerful cost savings enabled by HCF are realized in the 'avoided costs of CF' at the composite manufacturer level. A typical 700 bar compressed hydrogen Type 4 COPV system requires 75 kg of T700S conventional CF at $25.70/kg, costing $1927.50 in CF. The exact same system, using the targeted HCF with 44% open area, would only require (75 kg) x (1 – 0.44) = 42 kg, or 56% the mass of solid CF. Factoring in the 16.8% reduction in HCF manufacturing cost ($21.38/kg), only $897.96 in HCF is needed. Together, this accounts for a 53% reduction in CF costs to fabricate the exact same COPV system, resulting in an **'effective' HCF cost of $11.97/kg**. Moreover, the HCF COPV would weigh approximately 30% less (at 60% fiber volume fraction), which will have beneficial implications for final storage costs in $/kWh.

Achieving small dimension HCF is challenging, but our results thus far are very promising. Additionally, there is room to allow for slightly larger OD or smaller ID HFs, which would be easier to produce, and would remain close to the $12-15/kg cost target. If we define R as:

$$R = \frac{\text{hollow fiber annulus area}}{\text{reference solid fiber area}} = \frac{(OD_h^2 - ID_h^2)}{OD_s^2} \qquad (1)$$

$$R = \frac{m_h}{m_s} = \frac{LD_h}{LD_s} = \frac{\sigma_{eff}}{\sigma_{AN}} = \frac{E_{eff}}{E} \qquad (2)$$

where the subscripts h and s denote hollow and solid, respectively, and m, LD, σ, and E are mass, linear density, strength, and modulus - assuming equivalent strain to failure of the hollow and solid CF. Assuming the true density of the carbon comprising the solid and hollow CF remains constant at approximately 1.8 g/cc, R represents their ratio of masses. Given CF costs are on a per mass basis, the 'avoided CF cost' savings in composites is simply (1-R) x 100%. This allows us to calculate the effects of varying the HF dimensions, in terms of avoided costs. **Figure 9** plots the HCF wall thickness versus outer diameter, at varying avoided cost saving percentages relative to the solid 7 µm CF. The shaded green triangle in the **Figure 9** represents the window of HCF dimensions of interest, with corners located near 7/4.65 µm, 7/4.35 µm, and 10/8.1 µm OD/ID. The

latter two HCFs would offer an avoided CF cost of 30%, for an effective cost of $14.97/kg. Per equation (2), the three targeted HCFs identified would need to attain true break stresses (force/annulus area) of 8.77, 7.98 and 6.98 GPa, respectively to maintain the effective fiber strength of 4.9 GPa (T700S). Similarly, the true moduli would need to be 412, 375, and 328 GPa respectively, at 2.1 % strain to failure, to maintain an effective modulus to 230 GPa (T700S). Although these values are high for conventional PAN-based CF they are achievable. For example, T1000G has a strength and modulus of 7.0 and 324 GPa at 2 % strain to failure, and high modulus PAN-based fibers like M46J, at 436 GPa, already commercially exist. **In sum, this new cost model demonstrates that our PAN-based HCF approach offers effective CF costs between $12/kg and $15/kg – if we could achieve the target filament dimensions.**

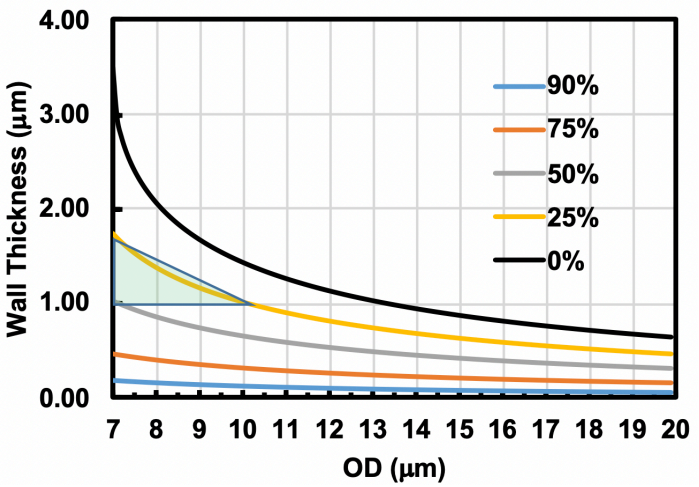

Figure 9. The HCF wall thickness as a function of outer diameter for varying avoided CF cost savings percentages (relative to a 7 µm solid CF).

Conclusions and Future Directions

A new terpolymer polyacrylonitrile, TechPAN, was shown to produce T700S CF quality properties (4.9 GPa strength, 230 GPa modulus) and represented a path to lower the polymer precursor, offering a 13% cost reduction in the final carbon fiber (in $/kg CF). The use of activated carbon for solvent capture from the wash water reduced fresh water usage, resulting in a 90% reduction in total effluent (wash water and solvent) to distillation. However, the AC lost 2.4% in specific surface area per thermal regeneration cycle. In sum, the use of activated carbon sorption during fiber spinning could reduce the resulting CF cost by an additional 8% if an AC with 0.02% surface area loss on regeneration was achieved. Multifilament tow hollow PAN precursors were successfully spun utilizing a segmented arc spinneret and a solution spinning technique. The continuous 25 filament fiber tows contained HF with concentric hollow cross sections. Fiber tows initially contained macrovoids stemming from the 100% water coagulation bath, but further work enabled spinning into a 30 wt.% DMSO/water coagulation bath, which demonstrated vastly reduced macrovoid content. The HF precursors attained an effective stress at break of 485 ± 56 MPa and an effective elastic modulus of 11 ± 0.7 GPa – very similar to the solid fiber baseline. Both batch and continuous oxidation of HF were evaluated. Results indicated that HFs experienced oxygen diffusion from the outside and from the inside, simultaneously. The conjugated oxidized

outer layer of the HF measured 4 μm in thickness and the inner thickness varied as a function of HF percent open area, with data suggesting a 4 μm oxidized inner layer thickness could be achieved in HF with approximately 50% open area. Overall, these results suggest that a HF with a wall thickness of 8 μm may prevent the formation of a skin-core structure. When comparing HF and solid fiber oxidation rates, it was found that HF increased in density faster compared to a solid fiber of similar outer diameter. Continuous oxidation of long length of HF (100s of m) proved the ability of the HF to retain its hollow structure despite the rigors of continuous oxidation. Additionally, despite the increased length, the HF sampled from the end of the length of tow and from the middle of the length of tow both experienced oxidation from the interior and exterior. Oxidized HF were successfully carbonized to form HCF. The resulting HCF had a 35 μm OD, 25 μm ID, and 5 μm wall thickness. To date, the highest HCF effective tensile strength was 880 MPa, with an effective modulus of 142 GPa, and tensile strain of 0.6%. Upon cost analysis, it was found that the technologies investigated here could reduce the effective CF cost from $29.40/kg to $12-15/kg – if the targeted HCF dimensions could be achieved (nominally 7/4.65 μm OD/ID). Moreover, we predict significant increases in HCF tensile properties stemming from such smaller dimension precursor fibers. Achieving stable multifilament spinning of such fibers is a major future technical goal.

Special Recognitions & Awards/Patents Issued

None

Publications/Presentations

1. “Insights into the relation between yield point, plastic modulus and degree of crystallinity of PAN Precursor Fiber”, Ruben Sarabia-Riquelme, Nik Hochstrasser, Ashley Morris and Matthew Weisenberger, Center for Applied Energy Research, University of Kentucky. 2540 Research Park Dr., Lexington, KY 40511, USA, presented at CARBON 2018, the international carbon conference in Madrid July 1 – 6, 2018.
2. DOE FC TechTeam meeting (Detroit/WebEx): 16 - 17 May 2018
3. DOE AMR Meeting, Washington DC: 13 – 15 June, 2018
4. Morris, E. Ashley, Nik Hochstrasser, Jordan Burgess, Ruben Sarabia-Riquelme, Anne Oberlink, and Matthew C. Weisenberger. 2019. "The importance of precursor fiber in the production of high-quality carbon fibers and composites." Carbon Fibers and Composites Workshop, Oak Ridge, TN, July 2019.
5. Morris, E. Ashley, Nik Hochstrasser, Jordan Burgess, Ruben Sarabia-Riquelme, Anne Oberlink, and Matthew C. Weisenberger. 2019. "Progress on the development of small diameter hollow PAN precursor and resultant carbon fibers." Carbon 2019, Lexington, KY, July 2019.
6. Ruben Sarabia-Riquelme, Emil Hochstrasser, E. Ashley Morris, David Eaton and Matthew C. Weisenberger. 2019. “Drastically Reduced Waste-Water Generation During Solution Spinning of PAN Fibers Using an Activated Carbon Solvent sorption System”, Carbon 2019, Lexington, KY, July 2019.

7. E.A. Morris, R. Sarabia-Riquelme, N. Hochstrasser, J. Burgess, A.E. Oberlink, D.L. Eaton, M.C. Weisenberger, Early development of multifilament polyacrylonitrile-derived structural hollow carbon fibers from a segmented arc spinneret, Carbon. In review (2021).

References

[1] G. Ordaz, C. Houchins, T. Hua Onboard type IV compressed hydrogen storage system - cost and performance status 2015; DOE hydrogen and fuel cells program record: 2015; pp 1-13.
[2] DOE Office of Energy Efficiency and Renewable Energy Fuel Cell Technologies Office Annual FOA, 2016. https://eere-exchange.energy.gov/.
[3] C.D. Warren Development of low cost, high strength commercial textile precursor (PAN-MA); ORNL: 2014.
[4] G. Zhou, Y. Liu, L. He, Q. Guo, H. Ye, Microstructure difference between core and skin of T700 carbon fibers in heat-treated carbon/carbon composites, Carbon 49(9) (2011) 2883-2892. 10.1016/j.carbon.2011.02.025
[5] E.A. Morris, M.C. Weisenberger, M.G. Abdallah, F. Vautard, H. Grappe, S. Ozcan, F.L. Paulauskas, C. Eberle, D. Jackson, S.J. Mecham, A.K. Naskar, High performance carbon fibers from very high molecular weight polyacrylonitrile precursors, Carbon 101 (2016) 245-252. DOI:10.1016/j.carbon.2016.01.104
[6] S.-P. Rwei, Formation of hollow fibers in the melt-spinning process, J. Appl. Polym. Sci. 82(12) (2001) 2896-2902. 10.1002/app.2145
[7] V. Grobe, K. Meyer, Faserforsch. Textiltech. 10 (1959) 214-224.
[8] L. Kong, H. Liu, W. Cao, L. Xu, PAN fiber diameter effect on the structure of PAN-based carbon fibers, Fibers Polym 15(12) (2015) 2480-2488. 10.1007/s12221-014-2480-1
[9] M.-J. Yu, C.-G. Wang, Y.-J. Bai, M.-X. Ji, Y. Xu, SEM and OM study on the microstructure of oxidative stabilized polyacrylonitrile fibers, Polym. Bull. (Berlin) 58(5-6) (2007) 933-940.
[10] M.-Y. Lv, H.-Y. Ge, J. Chen, Study on the chemical structure and skin-core structure of polyacrylonitrile-based fibers during stabilization, J. Polym. Res. 16(5) (2008) 513-517. 10.1007/s10965-008-9254-7
[11] T. Sun, Y. Hou, H. Wang, Effect of atmospheres on stabilization of polyacrylonitrile fibers, Journal of Macromolecular Science, Part A 46(8) (2009) 807-815. 10.1080/10601320903004657
[12] A. Takaku, T. Hashimoto, T. Miyoshi, Tensile properties of carbon fibers from acrylic fibers stabilized under isothermal conditions, J. Appl. Polym. Sci. 30(4) (1985) 1565-1571. 10.1002/app.1985.070300421
[13] G.S. Bhat, F.L. Cook, A.S. Abhiraman, L.H. Peebles, New aspects in the stabilization of acrylic fibers for carbon fibers, Carbon 28(2-3) (1990) 377-385. 10.1016/0008-6223(90)90011-m
[14] D. Choi, H.-S. Kil, S. Lee, Fabrication of low-cost carbon fibers using economical precursors and advanced processing technologies, Carbon 142 (2019) 610-649. 10.1016/j.carbon.2018.10.028

Acronyms

UK CAER	University of Kentucky Center for Applied Energy Research
COPV	composite overwrapped pressure vessel
PAN	polyacrylonitrile
DMSO	dimethylsulfoxide
CF	carbon fiber
HF	hollow fiber (precursor)
HCF	hollow carbon fiber
AC	activated carbon